Dalton Transactions

An international journal of inorganic chemistry

www.rsc.org/dalton

Volume 41 | Number 38 | 14 October 2012 | Pages 11521–11908

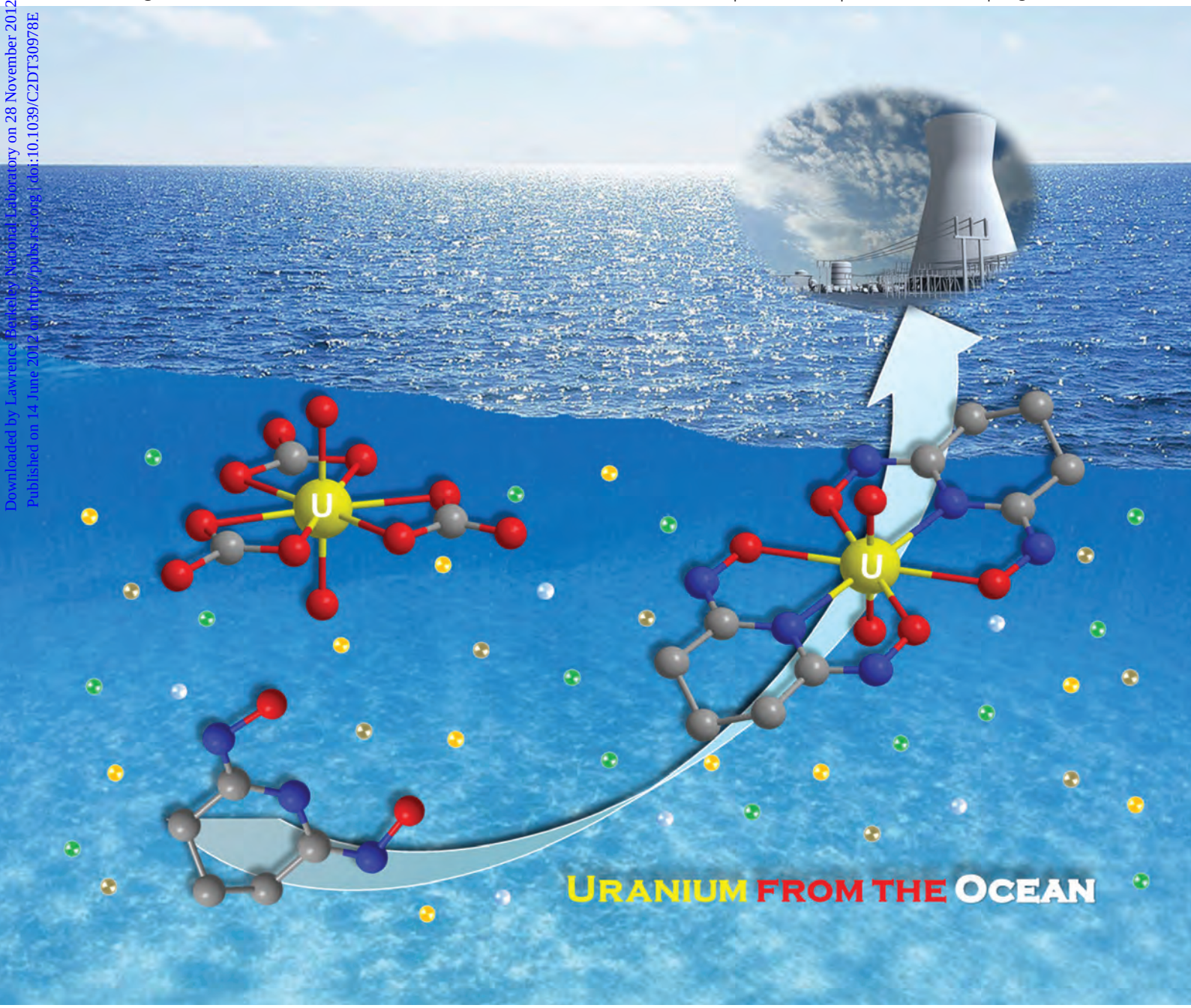

ISSN 1477-9226

RSC Publishing

COVER ARTICLE

Linfeng Rao *et al.*

Sequestering uranium from seawater: binding strength and modes of uranyl complexes with glutarimidedioxime

1477-9226(2012)41:38;1-J

Dalton Transactions

Dynamic Article Links
View Article Online

Cite this: *Dalton Trans.*, 2012, **41**, 11579

www.rsc.org/dalton

PAPER

Sequestering uranium from seawater: binding strength and modes of uranyl complexes with glutarimidedioxime†

Guoxin Tian,[a] Simon J. Teat,[b] Zhiyong Zhang[c] and Linfeng Rao*[a]

Received 4th May 2012, Accepted 13th June 2012
DOI: 10.1039/c2dt30978e

Glutarimidedioxime (H_2A), a cyclic imide dioxime ligand that has implications in sequestering uranium from seawater, forms strong tridentate complexes with UO_2^{2+}. The stability constants and the enthalpies of complexation for five U(VI) complexes were measured by potentiometry and microcalorimetry. The crystal structure of the 1 : 2 metal–ligand complex, $UO_2(HA)_2{\cdot}H_2O$, was determined. The re-arrangement of the protons of the oxime groups (–CH═N–OH) and the deprotonation of the imide group (–CH–NH–CH–) results in a conjugated system with delocalized electron density on the ligand (–O–N–C–N–C–N–O–) that coordinates to UO_2^{2+} *via* its equatorial plane.

Introduction

The concentration of uranium in the ocean is extremely low (3.3 μg L^{-1}). However, the total amount of uranium in the ocean is about 4.5 billion tons, a thousand times as much as the amount of uranium in terrestrial ores, because of the huge volume of seawater (1.4×10^9 km^3).[1,2] Therefore, the ocean is an important source of uranium if it can be extracted economically. Extraction of uranium from seawater is very challenging, not only because it is in an extremely low concentration, but also because it exists in seawater as very stable carbonate complexes[2] in the presence of many other metal ions (Na, K, Ca, Mg, Al and transition metals), some of which are in overwhelmingly higher concentrations.

Since the 1960s, various techniques have been studied and developed for the extraction of uranium from seawater, including solvent extraction, ion exchange, sorption with biomass, metal oxides (*e.g.*, TiO_2) and functionalized sorbents.[2–6] Among these, the Japanese process using amidoxime-based sorbents prepared by radiation grafting showed the most promise.[5,6] A sorption efficiency of 1.5 g U kg^{-1} sorbent was achieved in 30-day marine tests and the estimated cost was \$500 kg^{-1} uranium, about 2–3 times the spot market price of uranium.[1] These results could justify the further development of industrial scale marine systems to extract uranium from seawater at a price competitive with those from conventional uranium resources. Critical aspects for improvements include higher efficiency, higher selectivity and the recyclability of the sorbent.

A better understanding of the coordination modes and binding strength of the amidoxime group with uranium is the key to improving the extraction efficiency and selectivity. Unfortunately, very limited information on the complexation of uranium with amidoxime is available in the literature and the nature of the uranium–amidoxime complex has not been clearly illustrated. For example, the amidoxime group $–C(NH_2)NOH$ is expected to form a chelate complex with metal ions *via* the nitrogen atom of the amino group ($–C(NH_2)$) and the oxygen atom of the deprotonated $–C(NO^-)$ group. Crystal structures of some amidoxime complexes with transition metals (Co, Ni, Cu, Mo and Pt) have confirmed the formation of such chelate complexes.[7–14] However, the amidoxime ligand was found to be monodentate in the crystals of two amidoxime complexes with UO_2^{2+}, where the amino group ($–C(NH_2)$) does not coordinate to UO_2^{2+}.[15,16]

Based on early studies using functionalized ion exchange resins,[17,18] we have hypothesized that two types of amidoxime groups could form in the preparation of the sorbent, a cyclic imide dioxime and an open-chain diamidoxime (Scheme 1), and

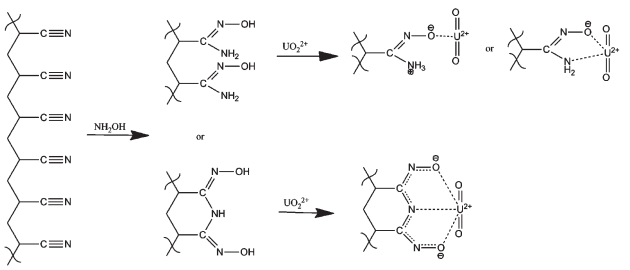

Scheme 1 A schematic of the idealized formation of open chain diamidoxime (upper) and cyclic imide dioxime (lower), and the possible coordination modes with UO_2^{2+}.

[a]*Chemical Sciences Division, Lawrence Berkeley National Laboratory, 1 Cyclotron Rd., Berkeley, California 94720, USA. E-mail: lrao@lbl.gov; Fax: +1 01 5104865596; Tel: +1 01 5104865427*
[b]*Advanced Light Source, Lawrence Berkeley National Laboratory, 1 Cyclotron Rd., Berkeley, California 94720, USA*
[c]*Stanford Nanofabrication Facility, Stanford University, Stanford, California 94305, USA*

†CCDC 859853 and 859445. For crystallographic data in CIF or other electronic format see DOI: 10.1039/c2dt30978e

that the cyclic imide dioxime could be more effective than the open-chain diamidoxime for complexing UO_2^{2+} because the former can afford tridentate coordination (Scheme 1). To test this hypothesis and help to improve the efficiency and selectivity of amidoxime-based sorbents for sequestering uranium, a small molecular ligand, glutarimidedioxime was synthesized and used as the water-soluble surrogate of the cyclic imide dioxime on the sorbent. The conditions for synthesizing the ligand were optimized. Its binding strength with UO_2^{2+}, the enthalpy of complexation and the coordination modes in the uranyl glutarimidedioxime complexes were investigated by multiple techniques, including potentiometry, spectrophotometry, microcalorimetry, single crystal X-ray diffraction and DFT calculations. In addition, the ability of glutarimidedioxime to compete with carbonate for binding UO_2^{2+} under seawater conditions was evaluated by spectrophotometry.

Experimental

Chemicals

All chemicals were reagent-grade or higher. Hydroxylamine (50 wt% solution in water, Aldrich) and glutaronitrile (99%, Sigma-Aldrich) were used as received. Boiled Milli-Q water was used in the preparation of all solutions. All experiments were conducted at 25 °C and an ionic strength of 0.5 M (NaCl), close to the seawater condition of 3% NaCl. The stock solution of U(VI) was prepared by dissolving UO_3 into HCl. The concentrations of U(VI) and free H^+ in the stock solution were determined, respectively, by fluorimetry[19] using standard solutions of U(VI) in 1 M H_3PO_4 and by the Gran titration.[20]

Ligand synthesis

A procedure in the literature[21–23] (Scheme 2) was adopted and optimized to prepare the ligand. Using the same starting materials at the molar ratio of 1 : 2 (glutaronitrile and hydroxylamine), different ligands (the cyclic glutarimidedioxime and the open chain glutardiamidoxime, named as H_2A and H_2B, respectively) could be prepared by controlling the reaction temperature. To obtain H_2A in high yields, 9.4 g glutaronitrile (99%) and 14.5 g hydroxylamine (50% in H_2O) were dissolved in 200 ml of 1/1 (*v*/*v*) ethanol/water and reacted at 80–90 °C with stirring for 5 days, resulting in H_2A as a white solid with >90% yield.

Ligand H_2A was characterized by ^{1}H-NMR: H_2A (pyridine-d_5), $-CH_2-CH_2-CH_2-$, 1.61 ppm, 2H; $-CH_2-CH_2-C(NOH)$ NH–, 2.49 ppm, 4H; –C(NOH)N***H***–C(NOH)–, 9.52 ppm, 1H; $-CH_2-C(NOH)NH-$, 12.16 ppm, 2H. The crystal structure of H_2A was also obtained by single-crystal X-ray diffractometry. The purity of H_2A was determined to be >99.5% with ^{1}H-NMR and potentiometry by titrating the H_2A solution with standard NaOH.

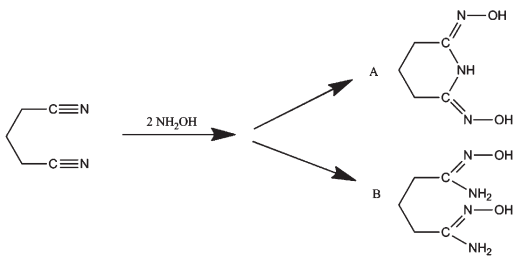

Scheme 2 Preparation routes for glutarimidedioxime (upper) and glutardiamidoxime (lower).

Potentiometry

The electrode potential (*E*, in millivolts) was measured with a Metrohm pH meter (Model 713) equipped with a Ross combination pH electrode (Orion Model 8102) in an inert atmosphere (Ar). The original inner solution (3 M KCl) of the electrode was replaced with 1 M NaCl. Prior to each titration, an acid–base titration with standard HCl and NaOH solutions was performed to obtain the electrode parameters, which allowed the calculation of hydrogen ion concentrations from the electrode potential in the subsequent titration. Multiple titrations were conducted with solutions of different concentrations of U(VI) (C_U as total [U(VI)]), ligand (C_A for the total ligand concentration, including H_2A, HA^- and A^{2-}) and acidity (C_H for total hydrogen ion, where $-C_H = C_{OH}$). For determining the protonation constant of the ligand, 20 mL of the ligand solution (C_A = 0.01–0.02 M; C_H = −0.02 to −0.04 M), were titrated with 1.0 M HCl. 50–100 data points were collected in each titration. For determining the stability constants of the U(VI) complexes, 20 mL of U(VI)/H_2A solutions (C_U: 0.20–0.50 mM; C_H: 2.0–4.0 mM: C_A: 1.0–2.0 mM) were titrated with 0.100 M NaOH. About 40–50 data points were collected for each titration. The protonation constants of the ligand and the stability constants of U(VI) complexes were calculated using the nonlinear regression program Hyperquad 2008.[24]

Spectrophotometry

Spectrophotometric titrations of U(VI) were carried out on a Cary 6000i spectrophotometer (Varian Inc.) from 350 to 200 nm with an interval of 0.5 nm. Two types of titrations were performed: (1) a U(VI) solution was titrated with the buffered ligand solution; (2) a solution containing both U(VI) and the ligand was titrated with HCl. After each addition of the titrant, the solution was mixed thoroughly (for 1–2 min) before the spectrum was collected. Preliminary kinetic experiments showed that the complexation reaction was fast and the absorbance became stable within 30 s of mixing. Usually, 15–20 additions were made, generating a set of 16–21 spectra in each titration.

Microcalorimetry

Calorimetric titrations were conducted at 25 °C with an isothermal microcalorimeter (Model: ITC 4200, Calorimetry Sciences Corp.) to determine the enthalpy of the reactions. Procedures and results of the calibration of the calorimeter are provided elsewhere.[25] Multiple titrations with different concentrations of U(VI), ligand and acidity were performed to reduce the uncertainty of the results. For the protonation of the ligand, 0.9 mL solution containing the ligand was placed in the reaction cell and titrated with 0.1 M HCl. For the complexation of U(VI) with the

Table 1 Crystal data and structure refinement

Identification code	$UO_2(HA)_2(H_2O)$	H_2A
Chemical formula	$C_{10}H_{18}N_6O_7U$	$C_5H_9N_3O_2$
Formula weight	572.33	143.15
Temperature	150(2) K	100(2) K
Radiation, wavelength	synchrotron, 0.77490 Å	synchrotron, 0.77490 Å
Crystal system, space group	orthorhombic, *Pccn*	orthorhombic, *Pbam*
Unit cell parameters	a = 13.0453(11) Å, α = 90° b = 13.9325(12) Å, β = 90° c = 8.0331(7) Å, γ = 90°	a = 7.1205(7) Å, α = 90° b = 14.1467(13) Å, β = 90° c = 13.5789(12) Å, γ = 90°
Cell volume	1460.0(2) Å^3	1367.8(2) Å^3
Z	4	8
Calculated density	2.604 g cm^{-3}	1.390 g cm^{-3}
Absorption coefficient m	6.020 mm^{-1}	0.109 mm^{-1}
F(000)	1072	608
Crystal color and size	Pale brown, 0.04 × 0.03 × 0.01 mm^3	Colorless, 0.20 × 0.06 × 0.02 mm^3
Reflections for cell refinement	7191 (θ range 4.55–33.48°)	7149 (θ range 3.12–33.36°)
Data collection method	Bruker APEX II CCD diffractometer ω rotation with narrow frames	Bruker APEX II CCD diffractometer ω rotation with narrow frames
q range for data collection	4.55–33.60°	3.14–33.07°
Index ranges	h −18–18, k −19–19, l −11–11	h −10–10, k −19–19, l −18–18
Completeness to q = 33.60°	99.8%	99.8%
Reflections collected	31 749	32 395
Independent reflections	2227 (R_{int} = 0.0734)	2072 (R_{int} = 0.0328)
Reflections with $F^2 > 2s$	1447	1769
Absorption correction	semi-empirical from equivalents	semi-empirical from equivalents
Min. and max. transmission	0.74 and 0.88	0.94 and 0.95
Structure solution	direct methods	direct methods
Refinement method	full-matrix least-squares on F^2	full-matrix least-squares on F^2
Weighting parameters a, b	0.0119, 4.2956	0.0627, 0.6130
Data/restraints/parameters	2227/2/146	2072/0/111
Final R indices [$F^2 > 2s$]	R_1 = 0.0258, wR_2 = 0.0565	R_1 = 0.0446, wR_2 = 0.1290
R indices (all data)	R_1 = 0.0437, wR_2 = 0.0650	R_1 = 0.0508, wR_2 = 0.1336
Goodness-of-fit on F^2	1.038	1.145
Largest and mean shift/su	0.001 and 0.000	0.000 and 0.000
Largest diff. peak and hole	1.531 and −0.590 e Å^{-3}	0.449 and −0.185 e Å^{-3}

ligand, 0.9 mL solution containing U(VI), the ligand and H^+ was titrated with a solution of NaOH. Usually, n additions (0.005 mL each) of the titrant were made through a 0.250 mL syringe, resulting in n experimental values of total heat ($Q_{ex,j}$, j = 1 to n, n = 40–50). These values were corrected for the heats of titrant dilution ($Q_{dil,j}$) that were measured in a separate run. The net reaction heat at the jth point ($Q_{r,j}$) was obtained from the difference: $Q_{r,j} = Q_{ex,j} - Q_{dil,j}$. The value of $Q_{r,j}$ is a function of the concentrations of the reactants (C_U, C_A and C_H), the equilibrium constants and the enthalpies of the reactions that occurred in the titration. These data, in conjunction with the protonation constants and the stability constants of U(VI) complexes obtained by potentiometry, were used to calculate the enthalpy of ligand protonation and complexation with U(VI) with the computer program HypDeltaH.[26]

Single-crystal X-ray diffractometry

Colorless crystals of H_2A were grown by recrystallization in water solutions. Pale brown crystals of the 1 : 2 (metal–ligand) complex, $UO_2(HA)_2(H_2O)$, were obtained by slow evaporation from 1 mL solution containing 1.0 mM UO_2^{2+} and 2.0 mM H_2A at pH 6–7. Representative crystals were mounted on the goniometer and crystallographic data were collected on the Small-Crystal Crystallographic Beamline 11.3.1 at the Advanced Light Source of Lawrence Berkeley National Laboratory (LBNL) using the Bruker APEX II CCD diffractometer of ω rotation with narrow frames at a wavelength of 0.77490 Å. Intensity data were collected within one hour using Bruker Apex 2 software.[27] Intensity data integrations, cell refinement and data reduction were performed using the Bruker SAINT software package.[28] Absorption correction was made with SADABS.[29] Dispersion factors (f' and f'') at 16 keV for C, N, O and U atoms were calculated using CROMER for Windows.[30] The structure was solved with direct methods using SHELXS and refined using SHELXL.[31] Non-hydrogen atoms were refined anisotropically. For the H_2A compound, hydrogen atoms on carbon atoms were placed geometrically and refined using a riding model. All other hydrogen atoms were found in the difference map and allowed to refine freely. For the compound $UO_2(HA)_2(H_2O)$, the hydrogen atoms were found in the difference map and allowed to refine freely, except for those on the water molecules that are restrained and refined using a riding model. Details of the crystallographic data are provided in Table 1.

DFT calculation

Density Functional Theory (DFT) calculations with relativistic core potentials (RECP) were carried out to get the information on the electronic interactions in the U(VI) complex, $UO_2(HA)_2$. Starting from the geometry obtained from the crystal structure of $UO_2(HA)_2(H_2O)$ in C_i symmetry, without including the water molecule, the calculations were performed with the generalized gradient approximation exchange and correlation functional

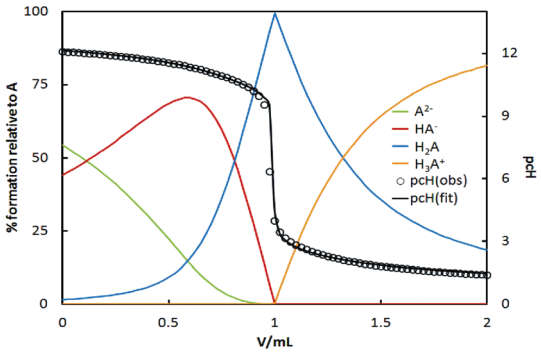

Fig. 1 Protonation titration of glutarimidedioxime. Initial cup solution: $V = 20$ mL, $C_A = 0.016$ M, $C_H = -0.018$ M. Titrant: 1 M HCl.

using the NWChem program suite.[32,33] We used the Stuttgart_RSC_1997_ECP effective core potential and basis set for U, and the Stuttgart_RLC_ECP effective core potential and basis set for C, N and O, and the DZVP_(DFT_Orbital) basis set for H in the EMSL (Environmental Molecular Sciences Laboratory) Basis Set Library.[34,35]

Results

Protonation of glutarimidedioxime

Fig. 1 shows a representative potentiometric titration for the protonation of glutarimidedioxime. The titration curve can be fitted with three steps of protonation, from A^{2-}, through HA^- and H_2A, to H_3A^+. The calculated protonation constants are listed in Table 2. The first stepwise protonation constant (12.06) is typical for the oxime group (–NOH).[36,37] The second stepwise protonation constant (10.7) is lower, indicating that the two oxime groups in H_2A are not completely independent and the protonation of one group reduces the basicity of the other group.[36] The low value of 2.1 for the third protonation step indicates that the imide group in H_2A is a weak base and it can only be protonated at low pH.

Complexation of U(VI) with glutarimidedioxime

Stability constants. Fig. 2 shows a representative potentiometric titration of the complexation of U(VI) with glutarimidedioxime. The best model to fit the potentiometric data includes the formation of five U(VI) complexes, UO_2HA^+, UO_2A, $UO_2(HA)_2$, $UO_2HA_2^-$ and $UO_2A_2^{2-}$, as represented by eqn (1):

$$UO_2^{2+} + mH^+ + nA^{2-} = UO_2H_mA_n^{(2n-m-2)-} \quad (1)$$

where $m = 0$, 1, or 2 and $n = 1$ or 2. The calculated stability constants for $UO_2H_mA_n^{(2n-m-2)-}$ are listed in Table 2.

Spectrophotometric titrations were also conducted to study the U(VI) complexation with glutarimidedioxime. Fig. 3a shows a titration of a U(VI) solution with the neutralized ligand, A^{2-}. Two significant changes in the spectra were observed as the ligand concentration was increased: (1) in the early part of the titration, two absorption bands at 230 and 280 nm appeared and increased; (2) after the ratio of the ligand to U(VI) reached 2, the intensity of the 280 nm band remained almost constant while that of the 230 nm band continued to increase. These features suggest that, as the ligand concentration was increased, U(VI)–H_2A complex(es) formed and the limiting species (in terms of the metal–ligand ratio) was the 1 : 2 U(VI)–H_2A complex(es).

Fig. 3b shows a titration of U(VI)–H_2A complexes with HCl. As the acidity was increased, the intensity of the 280 nm band decreased and that of the 230 nm band increased (with slight red-shifts). In comparison with the reference spectra of the ligand at different pH, the spectra changes in Fig. 3b indicate that the U(VI)–H_2A complexes dissociate in strongly acidic solutions due to the competition of H^+ with U(VI).

Efforts were made to calculate the stability constants of U(VI) complexes with glutarimidedioxime, but these proved to be unsuccessful. The reason for the failure probably lies in the fact that we were monitoring the absorption spectra of the ligand. The absorption spectra of the ligand in different U(VI) complexes, such as UO_2HA^+, UO_2A, $UO_2(HA)_2$, $UO_2HA_2^-$ and $UO_2A_2^{2-}$, may be too similar to be distinguished from each other.

Enthalpy of complexation. Fig. 4 shows a representative calorimetric titration of U(VI) complexation with glutarimidedioxime. The total reaction heat, $Q_{r,i}$, as well as the distribution

Table 2 Thermodynamic parameters of the protonation and complexation of glutarimidedioxime at 25 °C and 0.5 M ionic strength (NaCl)

Reaction	Log β	ΔH, kJ mol^{-1}	ΔS, J (K mol)$^{-1}$
$H^+ + A^{2-} = HA^-$	12.06 ± 0.23	−36.1 ± 0.5	110 ± 2
$2H^+ + A^{2-} = H_2A$	22.76 ± 0.31	−69.7 ± 0.9	202 ± 3
$3H^+ + A^{2-} = H_3A^+$	24.88 ± 0.35	−77 ± 6	218 ± 14
$UO_2^{2+} + A^{2-} = UO_2A$	17.8 ± 1.1	−59 ± 8	142 ± 19
$H^+ + UO_2^{2+} + A^{2-} = UO_2(HA)^+$	22.7 ± 1.3	−71 ± 6	197 ± 14
$UO_2^{2+} + 2A^{2-} = UO_2A_2^{2-}$	27.5 ± 2.3	−101 ± 10	188 ± 24
$H^+ + UO_2^{2+} + 2A^{2-} = UO_2(HA)A^-$	36.8 ± 2.1	−118 ± 6	309 ± 14
$2H^+ + UO_2^{2+} + 2A^{2-} = UO_2(HA)_2$	43.0 ± 1.1	−154 ± 25	307 ± 59

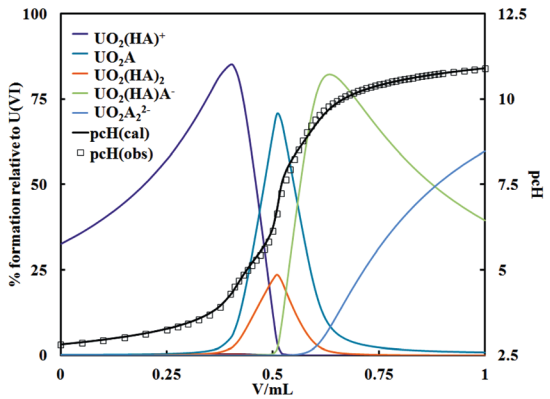

Fig. 2 Potentiometric titration for the complexation of H_2A with U(VI). Initial cup solution: $V = 20$ mL, $C_U = 0.5$ mM, $C_A = 1.25$ mM, $C_H = 4.06$ mM. Titrant: 0.1 M NaOH.

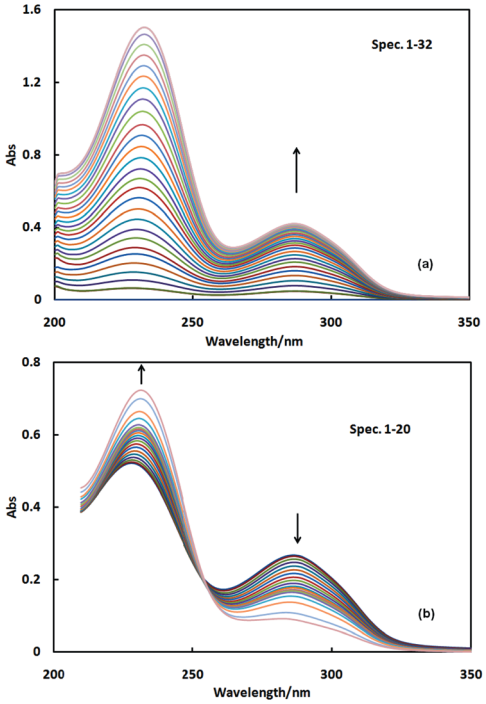

Fig. 3 Spectrophotometric titrations of complexation of U(VI) with H_2A. (a) Initial solution: V = 2 mL, C_U = 0.05 mM, C_H = 0.005 mM; titrant: C_A = 1 mM. (b) Initial solution: V = 2 mL, C_U = 0.0261 mM, C_H = 0.106 mM, C_A = 0.05 mM; titrant: C_H = 1.0 mM HCl.

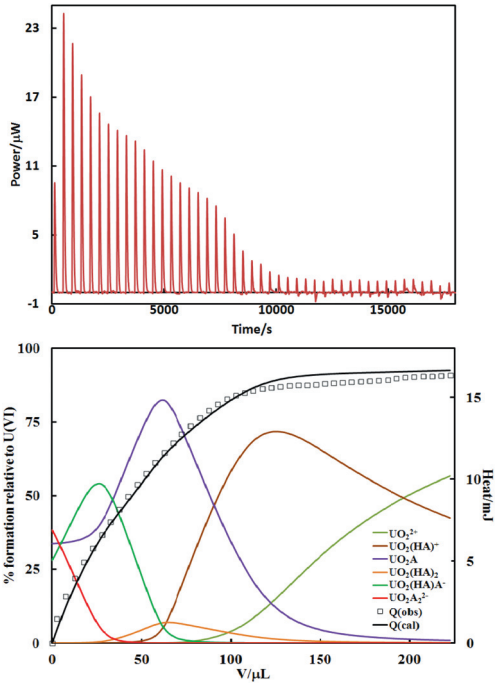

Fig. 4 Calorimetric titration of the complexation of U(VI) with H_2A at 25 °C. Initial solution: V = 0.9 mL, C_U = 0.6 mM, C_A = 1.0 mM, C_H = 0.11 mM; titrant: 0.01 M HCl, 5.0 μL per addition). (Upper) thermogram; (lower) total heat (right y axis) and speciation of U(VI) (left y axis) *vs.* the titrant volume.

of U(VI) species, is shown as a function of the titrant volume. From the reaction heat and the stability constants of the U(VI) complexes, the enthalpies, as well as the entropies of complexation were calculated and listed in Table 2.

Crystal structures of H_2A and $UO_2(HA)_2(H_2O)$

Single-crystal structures of the ligand H_2A and the neutral 1 : 2 UO_2^{2+}–HA^- complex, $UO_2(HA)_2H_2O$, are shown in Fig. 5. The U(VI) complex, $UO_2(HA)_2H_2O$, crystalized in a highly symmetrical structure with the *Pccn* space group symmetry. The uranium atom is at the center of inversion. The two HA^- ligands coordinate to the uranium center in a tridentate mode *via* the equatorial plane. The HA^- ligands are almost coplanar except for the middle methylene groups. The O═U═O moiety is perfectly linear and symmetrical, with an angle of 180° and typical U═O distances of 1.7846 Å.

Fig. 5 Crystal structures of H_2A (left) and $UO_2(HA)_2{\cdot}H_2O$ (right). 50% probability ellipsoids. All hydrogen atoms are found experimentally. The H_2O molecule is not shown for clarity.

Discussion

Electronic bonding interactions in $UO_2(HA)_2(H_2O)$

Two unusual and remarkable features are observed in the structure of the $UO_2(HA)_2$ complex: (1) the protons of both oxime groups (–CH═N–O**H**) are rearranged from the oxygen atom to the nitrogen atom; (2) the middle imide group (–CH–**N**H–CH–) is deprotonated, resulting in a −1 charged HA^{-1} ligand that coordinates to UO_2^{2+} in a tridentate mode (*via* the two oxime oxygen atoms and the imide nitrogen atom). With such configuration, the electron density on the HA^- ligand could actually be delocalized on –O–N–C–N–C–N–O–, forming a conjugated system that strongly coordinates to UO_2^{2+}. In fact, the bond length of the N–O bond of the oxime group is 1.42 Å in the H_2A molecule, but 1.35/1.36 Å in the $UO_2(HA)_2$ molecule (Fig. 5). The significant shortening of the N–O bond upon complexation with UO_2^{2+} supports the above arguments for a conjugated ligand system with delocalization of electron density on –O–N–C–N–C–N–O–.

DFT geometry optimization was carried out and the calculated bond lengths are compared with the experimental values in Table 3. For the U–O_3 (the axial O) and N_1–O_1 bonds, the difference between the calculated and the experimental is small (0.013 and 0.018 Å, respectively) and within the accuracy of typical DFT calculations. For the equatorial U–O_1, U–O_2 and U–N_3 bonds, the differences between the calculated and the experimental are −0.034, 0.066 and 0.128 Å, larger than those that can be explained by the uncertainties of DFT geometry optimization.

Crystal packing effects, if there are any, could probably be the reason for such relatively large differences.

The $UO_2(HA)_2$ complex can be formally described as $UO_2^{2+}(HA^-)_2$. For the UO_2^{2+} moiety, the Mulliken charges on the U and the axial O were calculated to be +0.51 and −0.07, respectively, indicating large donation of 1.63 e^- from the ligand to UO_2^{2+} and strong covalent bonding between UO_2^{2+} and HA^-. For the ligand HA^- in the $UO_2(HA)_2$ complex, the calculated Mulliken charges on the oxime O and imide N are −0.38 and −0.42, respectively. In comparison, the Mulliken charges on the oxime O and imide N in the free HA^- ligand are −1.03 and −0.66, respectively, again indicating the donation of significant electron density from the ligand to UO_2^{2+} and strong covalent bonding.

Two molecular orbitals (Fig. 6a and b) and an orbital energy diagram (Fig. 6c) are shown to illustrate the bonding interactions between UO_2^{2+} and the ligand (HA^-) moieties. The highest occupied orbitals of $UO_2(HA)_2$ can be divided into two sets, the upper and lower sets spanning an energy range of 1.9 eV and 1.2 eV respectively, as indicated by the two boxes with dotted lines (Fig. 6c). The upper set of orbitals of $UO_2(HA)_2$ are mostly non-bonding, essentially localized on the ligand moiety, with some contributions from the uranyl fδ and fφ orbitals as indicated by the dotted lines connecting the UO_2^{2+} and HA^- orbitals. The lower set of orbitals of $UO_2(HA)_2$ are mostly comprised of the bonding orbitals of uranyl (π_u, π_g, σ_u and σ_g) and the $1a_u$, $1a_g$, $2a_u$ and $2a_g$ orbitals of HA^-. Analysis of the calculated molecular orbitals indicates that the strongest bonding interactions between the ligand and uranyl are from the σ_u and σ_g orbitals on uranyl and the $2a_u$ and $2a_g$ orbitals on the ligands, as shown by the two molecular orbitals in Fig. 6a and b, and the energy diagram in Fig. 6c. The π_u and π_g orbitals of uranyl contribute to the bonding interactions, but only to a modest extent. The bonding interaction of the orbital in Fig. 6a results from the uranyl σ_u and ligand $2a_u$ orbitals. The interaction involves predominantly the ligand N lone pair p orbital with π character perpendicular to the ligand plane. The bonding interaction of the orbital in Fig. 6b, on the other hand, results from the uranyl σ_g and ligand $2a_g$ orbitals. The interaction predominantly involves the ligand N lone pair p orbitals, but with strong hybridization between the N p orbitals with σ and π character, in and perpendicular to the ligand plane, respectively. The analysis unambiguously shows the critical role of the orbitals on the imide N atom, particularly the orbitals with π character perpendicular to the ligand plane, in binding the uranyl. Maximizing the electron donating ability of the imide N atom should result in stronger interactions with uranyl.

Table 3 Comparison of bond lengths (Å) in $UO_2(HA)_2$ between the experimental and calculated (same atom labeling as in Fig. 5)

	U–O_3	U–O_1	U–O_2	U–N_3	N_1–O_1
Experimental	1.785	2.535	2.430	2.563	1.362
Optimized	1.798	2.501	2.495	2.691	1.380
Difference	0.013	—0.034	0.066	0.128	0.018

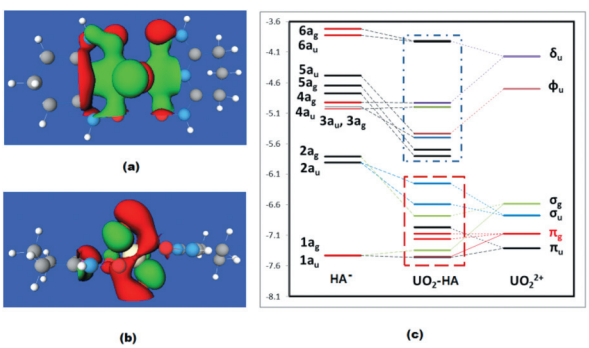

Fig. 6 Selected bonding orbitals in $UO_2(HA)_2$. (a) A strong bonding orbital between the uranyl σ_u and ligand $2a_u$; (b) a bonding orbital involving strong hybridization of the occupied σ and π orbitals on uranyl and hybridization between the N p orbitals in and perpendicular to the ligand plane; (c) the molecular orbital diagram.

The ability of glutarimidedioxime to compete with carbonate for the sequestration of U(VI) under seawater conditions

Under the conditions of seawater (pH ~ 8.3), the predominant species of uranium is the very stable tricarbonato U(VI) complex, $UO_2(CO_3)_3^{4-}$. Therefore, to be effective, the sequestering agent must be able to replace the carbonate in $UO_2(CO_3)_3^{4-}$. With the stability constants of U(VI) complexes with glutarimidedioxime from this work (Table 2) and with carbonate from the literature,[38] the speciation of U(VI) under seawater conditions (C_U = 3.3 ppb, $C_{carbonate}$ = 0.0023 M) is calculated with the speciation program associated with Hyperquad[24] and shown in Fig. 7. At the seawater pH (8.3) and in the presence of 0.001 M glutarimidedioxime, more than 95% U(VI) is complexed by glutarimidedioxime (86% $UO_2HA_2^-$, 8% $UO_2A_2^{2-}$, 2% UO_2A), while $UO_2(CO_3)_3^{4-}$ only accounts for 2% U(VI). This means that glutarimidedioxime is a much stronger complexant for U(VI) than carbonate at the seawater pH.

It should be emphasized that the speciation of uranium in seawater is much more complex than what is indicated in Fig. 7. As stated in the introduction section, many other metal ions (Na, K, Ca, Mg, Al and transition metals) exist in seawater and some of them are in overwhelmingly higher concentrations than uranium. They will compete with uranium for the sorption sites of the amidoxime-based sorbents. Therefore, the ability of

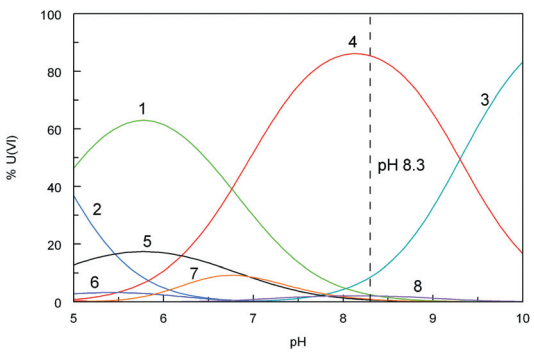

Fig. 7 Speciation of U(VI) (C_U = 3.3 ppb, $C_{carbonate}$ = 0.0023 M, C_A = 0.001 M). 1 – UO_2A, 2 – UO_2HA^+, 3 – $UO_2A_2^{2-}$, 4 – $UO_2HA_2^-$, 5 – $UO_2H_2A_2$, 6 – $UO_2(CO_3)$, 7 – $UO_2(CO_3)_2^{2-}$, 8 – $UO_2(CO_3)_3^{4-}$.

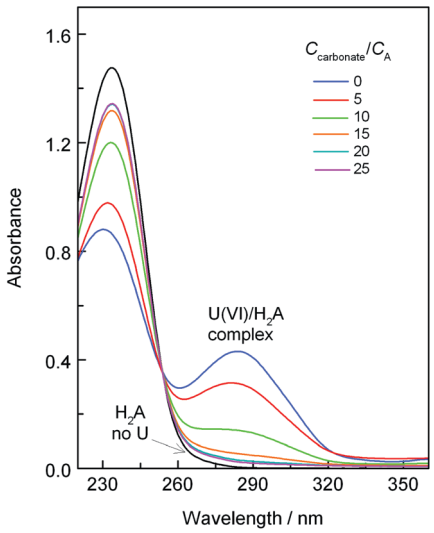

Fig. 8 Absorption spectra showing the competition of H_2A with carbonate for complexing uranium. C_U = 0.05 mM, except for one spectrum where C_U = 0 mM. C_A = 0.10 mM; $C_{carbonate}/C_A$ = 0–25; pH 8.1–8.3.

glutarimidedioxime to sequester U(VI) should be further evaluated in the presence of other major ions that exist in seawater. A study of the complexation of glutarimidedioxime with transition metals is under way.

Optical absorption spectra of U(VI) in the presence of glutarimidedioxime and carbonate were collected to further illustrate the competition between glutarimidedioxime and carbonate. As shown in Fig. 8, ligand H_2A absorbs very strongly in the UV region (an absorption band centered around 230 nm). The complexes with U(VI) have absorption bands around 280 nm. As the concentration of carbonate was increased, the intensity of the 280 nm band gradually decreased, but remained significantly strong even if the concentration of carbonate was 10 times as high as the concentration of glutarimidedioxime. This means that glutarimidedioxime can effectively compete with carbonate for complexing U(VI) at seawater pH conditions. It should be noted that the aqueous complexation experiments provide only qualitative evaluation of the ability of glutarimidedioxime for sequestering U(VI). When glutarimidedioxime is grafted on solid substrates, its effective concentration and ability of sequestering U(VI) could be higher than those observed in the above experiments.

Effect of temperature on the complexation

The temperature of seawater changes with locations, season and time, which could have significant impact on the efficiency of U(VI) sequestration from seawater if the sequestration reaction has strong temperature dependency. The enthalpies of complexation measured in this work allow the evaluation of the effect of temperature on the complexation of glutarimidedioxime with U(VI) under seawater conditions.

Based on the thermodynamic parameters on the speciation of carbonate,[37] glutarimidedioxime and its complexes with U(VI) (Table 2), the dominant species under seawater pH are HCO_3^-, H_2A, $UO_2(CO_3)_3^{4-}$ and/or $UO_2(HA)A^-$, respectively. Therefore, the major overall reaction can be written as:

$$UO_2(CO_3)_3^{4-} + 2H_2A = UO_2(HA)A^- + 3HCO_3^- \quad (2)$$

Using the enthalpy values for HCO_3^- and $UO_2(CO_3)_3^{4-}$ in the literature[37,38] and for H_2A and $UO_2(HA)A^-$ from this work (Table 2), the enthalpy of reaction (2) is calculated to be +16.7 kJ mol^{-1}. This means that the overall sequestration of U(VI) from seawater by glutarimidedioxime is endothermic, and that the efficiency of sequestration is enhanced at higher temperatures. This thermodynamic analysis confirms the observation in the marine experiments in Japan that the U(VI) extraction efficiency was higher from warmer seawaters.[5,6] The marine experiments in Japan showed a 1.5 times increase in the efficiency when the seawater temperature increased by 10 °C.[5,6] In fact, using the van't Hoff equation and the enthalpy of reaction (2) (+16.7 kJ mol^{-1}), it is estimated that the equilibrium constant of reaction (2) at 20 °C would be 1.3 times that at 10 °C, in excellent agreement with the observations in the marine experiments.

The enthalpies of complexation for the five U(VI) complexes with glutarimidedioxime are all negative (Table 2), but the enthalpy of reaction (2) is positive (unfavorable to the sequestration of U(VI) from seawater by glutarimidedioxime). One of the reasons for the endothermic enthalpy of reaction (2) is that the dissociation of $UO_2(CO_3)_3^{4-}$ is highly endothermic (+39.2 kJ mol^{-1}).[38] Based on this observation, we hypothesize that direct sorption of $UO_2(CO_3)_3^{4-}$ with an anionic sorbent could be favored by the enthalpy of reaction; a research area to be explored in future studies.

Summary

Glutarimidedioxime (H_2A) was synthesized with high yields by controlling the temperature of the reaction between glutaronitrile and hydroxylamine. It was studied as the small molecular water-soluble surrogate for the amidoxime-based sorbents that have been used for the sequestration of uranium from seawater. Glutarimidedioxime was found to form very strong tridentate complexes with UO_2^{2+}. At the seawater pH, glutarimidedioxime could effectively compete with carbonate for complexing UO_2^{2+}. The crystal structure of a 1 : 2 uranyl–ligand complex, $UO_2(HA)_2$, in conjunction with DFT calculations, reveals the coordination modes and the nature of the electronic interactions in $UO_2(HA)_2$.

Results from this work reveal that the unusual deprotonation of the imide group and the rearrangement of the protons in the oxime groups results in a large conjugated ligand system that strongly coordinates to UO_2^{2+} *via* its equatorial plane in a tridentate mode. This work also suggests that conducting the grafting/reaction process for preparing the sorbent at 80–90 °C helps to achieve high yields of glutarimidedioxime, a preferred cyclic imide dioxime ligand, and that increasing the electron donation ability of the imide nitrogen atom in glutarimidedioxime could significantly enhance the binding ability of the ligand towards UO_2^{2+}.

Acknowledgements

This work was supported by the Uranium Resources Program, Fuel Cycle Research and Development Program, Office of

Nuclear Energy of the U. S. Department of Energy (DOE) under Contract No. DE-AC02–05CH11231 at Lawrence Berkeley National Laboratory (LBNL). Single-crystal X-ray diffraction data were collected and analyzed at the Advanced Light Source (ALS). ALS is supported by the Director, Office of Science, Office of Basic Energy Sciences, U. S. DOE under Contract No. DE-AC02-05CH11231. The National Nanotechnology Infrastructure Network (NNIN) of Stanford University is acknowledged for computational resources. Dr. Chao Xu of Tsinghua University, Beijing, China, designed the artwork to be considered for the cover page of this publication.

Notes and references

1 OECD, Uranium 2009: Resources, Production and Demand, OECD NEA Publication 6891, 2010, 456.
2 R. V. Davies, J. Kennedy, R. W. McIlroy, R. Spence and K. M. Hill, *Nature*, 1964, **203**, 1110.
3 K. Schwochau, *Top. Curr. Chem.*, 1984, **124**, 91.
4 M. Kanno, *J. Nucl. Sci. Technol.*, 1984, **21**, 1.
5 T. Shimizu and M. Tamada, *Proceedings of Civil Engineering in the Ocean*, 2004, **20**, 617.
6 M. Tamada, N. Seko, N. Kasai and T. Shimizu, *Transactions of the Atomic Energy Society of Japan*, 2006, **5**, 358.
7 L. Malatesta, G. La Monica, M. Manassero and M. Sansoni, *Gazz. Chim. Ital.*, 1980, **110**, 113.
8 K. Wieghardt, W. Holzbach, E. Hofer and J. Weiss, *Chem. Ber.*, 1981, **114**, 2700.
9 D. L. Cullen and E. C. Lingafelter, *Inorg. Chem.*, 1970, **9**, 1865.
10 C. D. Stout, M. Sundaralingam and G. H. Y. Lin, *Acta CrystCrystallogr., Sect. B: Struct. Crystallogr. Cryst. Chem.*, 1972, **B28**, 2136.
11 Ö. Bekaroglu, S. Sarisaban, A. R. Koray, B. Nuber, K. Weidenhammer, J. Weiss and M. L. Ziegler, *Acta Crystallogr., Sect. B: Struct. Crystallogr. Cryst. Chem.*, 1978, **B34**, 3591–3593.
12 H. Endres, T. Jannack and B. Prickner, *Acta Crystallogr., Sect. B: Struct. Crystallogr. Cryst. Chem.*, 1980, **B36**, 2230.
13 H. Endres, *Acta Crystallogr., Sect. B: Struct. Crystallogr. Cryst. Chem.*, 1982, **B38**, 1313.
14 H. Endres and N. Genc, *Acta Crystallogr., Sect. C: Cryst. Struct. Commun.*, 1983, **C39**, 704.
15 E. G. Witte, K. S. Schwochau, G. Henkel and B. Krebs, *Inorg. Chim. Acta*, 1984, **94**, 323.
16 A. Zhang, T. Asakura and G. Uchiyama, *React. Funct. Polym.*, 2003, **57**, 67.
17 H. J. Schenk, L. Astheimer, E. G. Witte and K. Schwochau, *Sep. Sci. Technol.*, 1982, **17**, 1293.
18 L. Astheimer, H. J. Schenk, E. G. Witte and K. Schwochau, *Sep. Sci. Technol.*, 1983, **18**, 307.
19 C. W. Sill and H. E. Peterson, *Anal. Chem.*, 1947, **19**, 646.
20 G. Gran, *Analyst*, 1952, **77**, 661.
21 F. Eloy and R. Lenaers, *Chem. Rev.*, 1962, **62**, 155.
22 A. R. Forrester, H. Irikawa, R. H. Thomson, S. O. Woo and T. J. King, *J. C. S. Perkin I*, 1981, 1712.
23 J. A. Elvidge, R. P. Linstead and A. M. Salaman, *J. Chem. Soc.*, 1959, 208.
24 P. Gans, A. Sabatini and A. Vacca, *Talanta*, 1996, **43**, 1739.
25 L. Rao, T. G. Srinivasan, A. Yu. Garnov, P. Zanonato, P. Di Bernardo and A. Bismondo, *Geochim. Cosmochim. Acta*, 2004, **68**, 4821.
26 P. Gans, A. Sabatini and A. Vacca, *J. Solution Chem.*, 2008, **4**, 467.
27 Apex2: Bruker Analytical X-ray Systems Inc., Madison, WI, 2003.
28 *SAINT: SAX Area-Detector Integration Program v7.60a*, Bruker Analytical X-ray Systems, Inc., Madison, WI, 2010.
29 R. H. Blessing, *Acta Crystallogr., Sect. A: Fundam. Crystallogr.*, 1995, **A51**, 33.
30 W. L. Kissel and R. H. Pratt, *Acta Crystallogr., Sect. A: Fundam. Crystallogr.*, 1990, **A46**, 170.
31 G. M. Sheldrick, SHELXS-97, *Acta Crystallogr., Sect. A: Fundam. Crystallogr.*, 2008, **A64**, 112.
32 J. P. Perdew, K. Burke and M. Ernzerhof, *Phys. Rev. Lett.*, 1996, **77**, 3865.
33 M. Valiev, E. J. Bylaska, N. Govind, K. Kowalski, T. P. Straatsma, H. J. J. van Dam, D. Wang, J. Nieplocha, E. Apra, T. L. Windus and W. A. de Jong, *Comput. Phys. Commun.*, 2010, **181**, 1477.
34 W. Kühle, M. Dolg, H. Stoll and H. Preuss, *J. Chem. Phys.*, 1994, **100**, 7535.
35 EMSL Basis Set Library (http://www.emsl.pnl.gov/forms/basisform.html).
36 N. Durust, M. A. Akay, Y. Durust and E. Kilic, *Anal. Sci.*, 2000, **16**, 825.
37 A. E. Martell, R. M. Smith and R. J. Motekaitis, *NIST Critically Selected Stability Constants of Metal Complexes Data Base. NIST Stand. Ref. Database 46*, U. S. Department of Commerce, Gaithersburg, MD, 1998.
38 I. Grenthe, J. Fuger, R. J. Konings, R. J. Lemire, A. B. Muller, C. Nguyen-Trung and H. Wanner, *Chemical thermodynamics of uranium*, ed. H. Wanner and I. Forest, Elsevier Science Publishers B. V., Amsterdam, 1992.

